Supplementary Material

Using boundary layer equilibrium to reduce uncertainties in transport models and CO_2 flux inversions

I.N. Williams[1], W.J. Riley[2], M.S. Torn[2], J.A. Berry[3], and S.C. Biraud[2]

1 Department of Geophysical Sciences, University of Chicago, Chicago, IL, USA

2 Lawrence Berkeley National Laboratory, Earth Sciences Division, Berkeley, CA, USA

3 Carnegie Institution of Washington, Stanford, CA, USA

Correspondence to: Ian N. Williams (inw@uchicago.edu)

S1. Scaling relationship for mixed-layer tracer budgets

The scaling relationship developed in Section (3.1) predicts that the relative importance of different transport and mixing processes depends on the timescale of interest and on the boundary layer relaxation time. The relaxation time in turn varies according to the strength of the divergent circulation. To test this hypothesis we first reproduced the results of Fig. (2a,b) in a scatter plot where each point represents the sum of entrainment and storage (y-axis), and advection (x-axis), binned according to a given averaging time (Fig. S1a,d), and allowing for uneven bin spacing to ensure equal numbers of ensemble members in each bin. Fig. (S1a,d) reveals the same timescale dependence shown in Fig. (2), except the scatter plots additionally reveal the individual magnitudes of entrainment and storage, and advection, and their standard deviations (numbered labels in Fig. S1a,d represent mean averaging times for each bin).

We then calculated t^* using mixed layer depths and vertical velocities (H_o,W_o) averaged across the three sites (SGP, LEF, HFM), referred to here as t_o^*. We first binned the budget terms as in Fig. (S1a,d), but according to t_o^* as opposed to the averaging time. Typical values of t_o^* and t^* range from 1.5 to 0.01 for averaging times of 1 to 90 days, respectively. The results (Fig. S1) confirm that the ratio of entrainment plus storage to advection scales linearly with t_o. Differences in the slopes of the linear relations, particularly between HFM and the other two sites, are eliminated when scaled according to t^*, where the contribution of differences in local atmospheric circulation is taken into account (Fig. S1c,f) by calculating mixed layer depths and vertical velocities at each site.

S2. Relaxation times at HFM and LEF from CarbonTracker and ECMWF reanalyses

We calculated relaxation times in the CarbonTracker (CT/TM5) dataset at SGP, LEF, and HFM, as in Section 5. The difference between the summer and winter relaxation times at SGP and HFM is captured by the theoretical solution to the conservation equation (gray lines in Fig. S3), but the summer CT/TM5 concentration gradient at HFM decays faster than theory predicts (Fig. S3c). Note that the theoretical gray lines for SGP in Fig. (8a,b) are the same as those in Fig. (S3a,d), except for the addition of two years (2001, 2002) of data from the CT/TM5 analyses. Removing the additional two years had no effect on the agreement between observations, theory, and CT/TM5, seen by comparing panels (8a,b,) and (S3a,d). The disagreement between theory and CT/TM5 in summer at HFM (and in winter at LEF) did not improve upon changing the averaging time from 90 to 45 days or 180 days. These results indicate a discrepancy in vertical transport and mixing between CT/TM5 and ECMWF interim reanalysis datasets, which warrants future diagnostic studies using observed trace gas concentrations from the measurement towers at LEF and HFM.

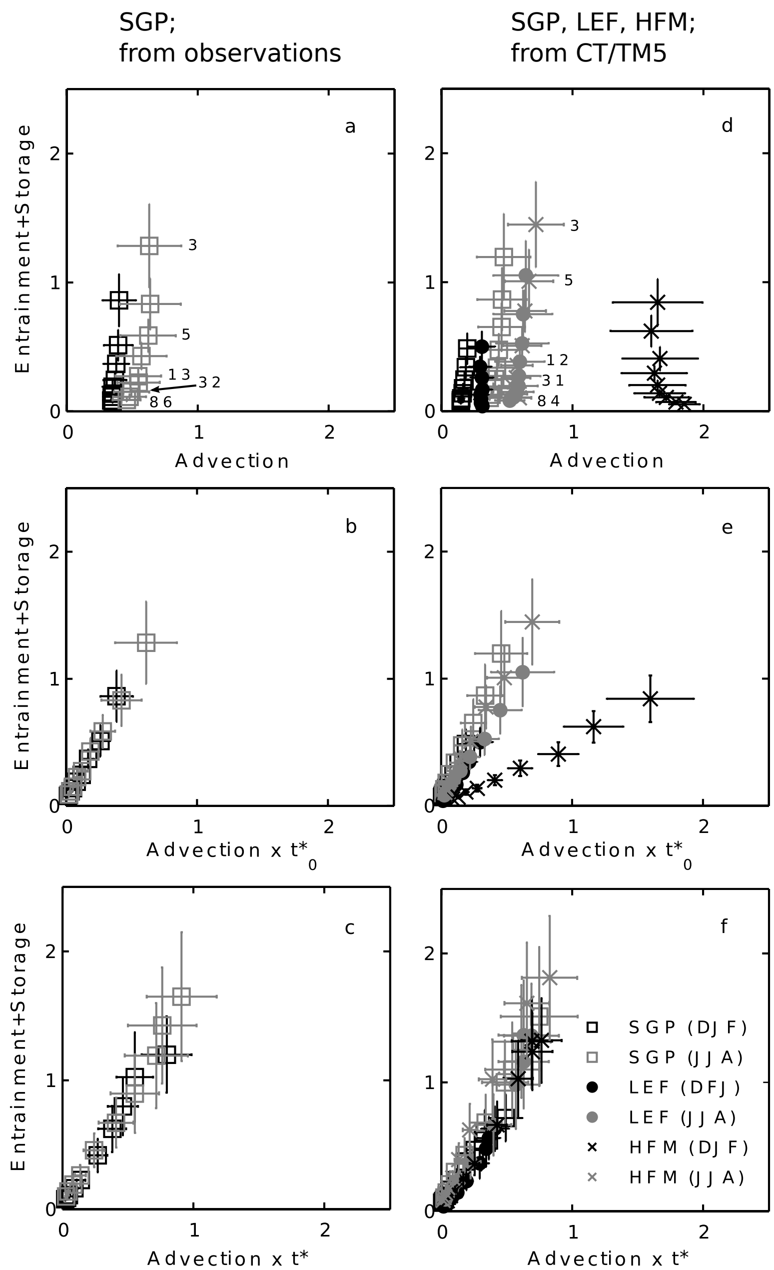

Fig. S1. Magnitudes of entrainment plus storage, and vertical advection (μmol mol^{-1}m^{-2}s^{-1}), based on observations at SGP (a,b,c), and on CT model output at SGP, LEF, and HFM (d,e,f). Values of entrainment, storage, and vertical advection, were binned according to the averaging time (a,d) or the non-dimensional numbers $t_o^*=H_oW_o^{-1}T^{-1}$ (b,e) and $t^*=HW^{-1}T^{-1}$ (c,f) (see Section 3.1 for definitions). Averaging was performed over each bin (width of cross bars gives half the standard deviation) and vertical advection was scaled according to each bin value in panels (b,c,e,f). A few representative averaging times are indicated in panels (a,d) for SGP and HFM for June-July-August.

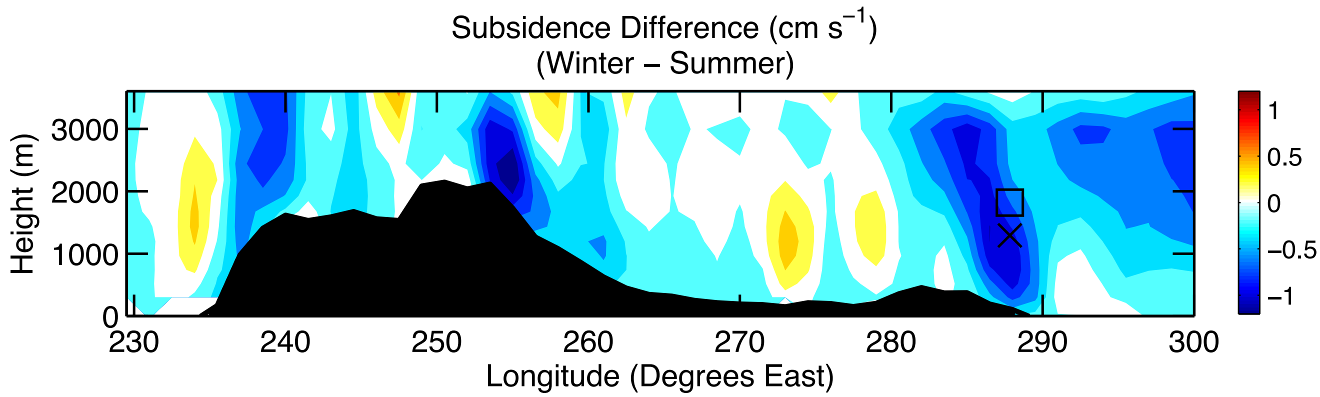

Fig. S2: Longitude-height cross-section showing the difference between winter and summer subsidence velocities at the latitude of HFM (height in meters above sea level). Negative values indicate greater subsidence (stronger descent) in winter than in summer. Subsidence is calculated by averaging the negative values of vertical velocity over each season (90-days). Black shading indicates the height of the surface topography. Symbols indicate summer (square) and winter (x) mixed-layer depth at the longitude of HFM. See discussion of these results in Section 4.

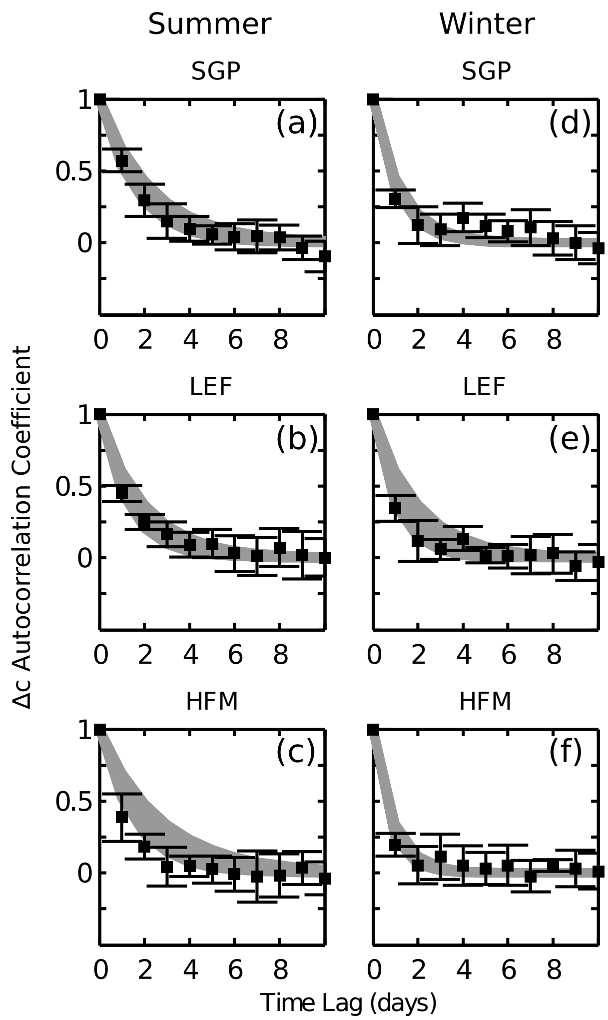

Fig. S3. As in Fig. (8) but using vertical concentration gradients from the CT model during winter at SGP (a), LEF (b), and HFM (c), and summer (d,e,f). This figure shows autocorrelation coefficients for perturbations (about 90-day averages) in daily vertical mixing ratio gradients, calculated for each year between 2003 and 2007 separately before averaging over all years. Error bars indicate the standard deviation of the mean over all years. The gray line indicates exponential decay toward the 90-day average value with rate constant t* (calculated from ECMWF interim-reanalysis vertical velocities).